

Kinetic Theory Based CFD Modeling of particulate Flows in Horizontal Pipes

Pandaba Patro and Brundaban Patro

Abstract—The numerical simulation of fully developed gas–solid flow in a horizontal pipe is done using the eulerian-eulerian approach, also known as two fluids modeling as both phases are treated as continuum and inter-penetrating continua. The solid phase stresses are modeled using kinetic theory of granular flow (KTGF). The computed results for velocity profiles and pressure drop are compared with the experimental data. We observe that the convection and diffusion terms in the granular temperature cannot be neglected in gas solid flow simulation along a horizontal pipe. The particle-wall collision and lift also play important role in eulerian modeling. We also investigated the effect of flow parameters like gas velocity, particle properties and particle loading on pressure drop prediction in different pipe diameters. Pressure drop increases with gas velocity and particle loading. The gas velocity has the same effect ((proportional to U^2) as single phase flow on pressure drop prediction. With respect to particle diameter, pressure drop first increases, reaches a peak and then decreases. The peak is a strong function of pipe bore.

Keywords—CFD, Eulerian modeling, Gas solid flow, KTGF.

I. INTRODUCTION

SOLIDS moving with a gas stream in a pipeline can be found in many industrial processes, such as power generation, chemical, pharmaceutical, food and commodity transfer processes. Horizontal gas solid flow simulation has always been a challenge due to gravity induced particle accumulation on the bottom wall and re-suspended by the gas flow. Hence particle–wall collision along with particle-particle collision dominate the flow phenomena [1]. The Euler-Euler method, also often named two-fluid model, treats the solid phase as a continuum interacting with the fluid continuum [2] and assumes that the particle assembly behaves like a fluid [3]. Basically, this approach has been developed for high solid concentrations, where individual particle tracking (Lagrangian approach) involves a lot of computational cost. Many researchers [4] – [9] investigated the hydrodynamics of gas solid flows using eulerian approach. They had shown that eulerian model is capable of predicting the flow physics of gas solid flows qualitatively as well as quantitatively.

In our investigation, we use eulerian modeling for the flow of a gas-particle mixture in a horizontal pipe with account the gravity force, particle-wall interaction, inter-particle collisions and lift forces. The lift forces are caused by particle rotation due to collisions with the bottom wall and a non-uniform gas velocity field. Predictions were made with the numerical

settings validated against bench mark experimental data by Tsuji et al. [10] We also do an extensive study on the effect of important flow parameters like inlet gas velocity, particle diameter, solid volume fraction, particle density on the pressure drop prediction in horizontal gas solid flow. Calculations were performed for relatively high particle mass concentrations (1% to 10% solid volume fraction) and different particle sizes (from 35 micron to 200 micron). The gas used is air at normal temperature and pressure. Basically most of the work on gas solid flow has been done in a constant diameter pipe, but here we consider different pipe diameters to investigate the gas solid flow.

II. FLOW PARAMETERS USED IN OUR STUDY

The influential parameters in predicting pressure gradient in pneumatic conveying are: density of solids (ρ_s) in kg/m^3 , volume fraction of solids (α), diameter of particles (d_p) in micron, inlet gas velocity (U) in m/s and pipe diameter (D) in mm.

The gas Reynold's number is defined as

$$Re_g = \frac{\rho_g U D}{\mu_g}$$

where D is the pipe diameter, ρ_g and μ_g are the density and dynamics viscosity respectively of gas phase. Particle loading or solids loading ratio (SLR) is defined as the ratio of mass flow rate of solid phase and mass flow rate of gas phase. In Fully developed state, the solid phase and gas phase velocity become approximately equal.

$$SLR = \frac{\alpha \rho_s}{(1 - \alpha) \rho_g}$$

III. GOVERNING EQUATIONS

In a two-fluid model, both the phases are treated as continuum. The governing equations for a dispersed solid phase and a carrier gas phase are locally averaged, and both expressions have the same general form. The gas phase momentum equation is closed using k- ϵ turbulence model. Solid phase stresses are modeled using kinetic theory [2].

The conservation equation of the mass of phase i (i=gas or solid) is

$$\frac{\partial}{\partial t}(\alpha_i \rho_i) + \nabla \cdot (\alpha_i \rho_i u_i) = 0 \quad (1)$$

P. Patro is with Department of Mechanical Engineering, IIT Kharagpur-721302, India (phone: +91-9002507605 e-mail: ppatro@mech.iitkgp.ernet.in).

B.Patro, is with Department of Mechanical Engineering NIT Rourkela-769008, India (e-mail: bpatro11@gmail.com).

$$\sum \alpha_i = 1$$

The conservation equation for the momentum of the gas phase is

$$\frac{\partial}{\partial t}(\alpha_g \rho_g \bar{u}_g) + \nabla \cdot (\alpha_g \rho_g \bar{u}_g \bar{u}_g) = -\alpha_g \nabla p + \nabla \cdot \bar{\tau}_g + \alpha_g \rho_g \bar{g} + K_{sg}(\bar{u}_s - \bar{u}_g) \quad (2)$$

The conservation equation for the momentum of the solid phase is

$$\frac{\partial}{\partial t}(\alpha_s \rho_s \bar{u}_s) + \nabla \cdot (\alpha_s \rho_s \bar{u}_s \bar{u}_s) = -\alpha_s \nabla p - \nabla p_s + \nabla \cdot \bar{\tau}_s + \alpha_s \rho_s \bar{g} + K_{gs}(\bar{u}_g - \bar{u}_s) \quad (3)$$

$K_{gs} = K_{sg}$ is the gas-solid momentum exchange coefficient
Stress-strain tensor is given by

$$\bar{\tau}_i = \alpha_i \mu_i (\nabla \bar{u}_i - \nabla \bar{u}_i^T) + \alpha_i \left(\lambda_i - \frac{2}{3} \mu_i \right) \nabla \cdot \bar{u}_i \bar{I} \quad (4)$$

The compressibility effect of gas phase is neglected and hence the bulk viscosity is assumed to be zero.

A. Drag Force Model

In gas-solid flow, the gas exerts drag on the solids for their transportation. There are different empirical drag force models available in literature. The gas-solid momentum exchange (drag force coefficient) uses the Gidaspow [2] model.

When $\alpha_g > 0.8$

$$K_{sg} = \frac{3}{4} C_D \frac{\alpha_s \alpha_g \rho_g}{d_p} \left| \bar{u}_s - \bar{u}_g \right| \alpha_g^{-2.65} \quad (5)$$

$$C_D = \frac{24}{\text{Re}_p} \left[1 + 0.15 (\text{Re}_p)^{0.687} \right], \text{Re}_p \leq 1000$$

$$= 0.44, \text{Re}_p > 1000$$

The particle Reynolds number is given by:

$$\text{Re}_p = \frac{\alpha_g \rho_g \left| \bar{u}_g - \bar{u}_s \right| d_p}{\mu_g}$$

When $\alpha_g < 0.8$.

$$K_{sg} = 150 \frac{\alpha_s (1 - \alpha_g) \mu_g}{\alpha_g d_p^2} + 1.75 \frac{\rho_g \alpha_s \left| \bar{u}_s - \bar{u}_g \right|}{d_p} \quad (6)$$

B. Constitutive Equations using KTGF

In the gas-solid flow, particle motion is dominated by the collision interactions. So Fluid kinetic theory can be applied to describe the effective stresses in solid phase to close the momentum balance equation.

Solid pressure is Pressure exerted on the containing wall due to the presence of Particles. Lun et al. [11] correlation for solids pressure is

$$p_s = \alpha_s \rho_s \theta_s + 2 \rho_s (1 + e_{ss}) \alpha_s^2 g_{o,ss} \theta_s \quad (7)$$

The radial distribution function is a correction factor that modifies the probability of collision close to packing. The model proposed by Lun et al. [11] is

$$g_{o,ss} = \left(1 - \left(\frac{\alpha_s}{\alpha_{s,\max}} \right)^{\frac{1}{3}} \right)^{-1} \quad (8)$$

Bulk viscosity accounts for the resistance of the solid body to dilation.

$$\lambda_s = \frac{4}{3} \alpha_s \rho_s d_p g_{o,ss} (1 + e_{ss}) \left(\frac{\theta_s}{\pi} \right)^{\frac{1}{2}} \quad (9)$$

Granular Shear viscosity due to kinetic motion and collisional interaction between particles is

$$\mu_s = \mu_{s,\text{coll}} + \mu_{s,\text{kin}}$$

By Gidaspow [2]:

$$\mu_{s,\text{kin}} = \frac{5 d_p \rho_s (\theta_s \pi)^{\frac{1}{2}}}{96 \eta g_{o,ss}} \left[1 + \frac{8}{5} g_{o,ss} \alpha_s \eta \right] \quad (10)$$

$$\mu_{s,\text{coll}} = \frac{8}{5} \alpha_s^2 \rho_s d_p g_{o,ss} \eta \left(\frac{\theta_s}{\pi} \right)^{\frac{1}{2}} \quad (11)$$

C. Granular Temperature:

Kinetic energy associated with the random motion of the particles results in the transport equation for the granular temperature.

$$\frac{3}{2} \left[\frac{\partial}{\partial t} (\rho_s \alpha_s \theta_s) + \nabla \cdot (\rho_s \alpha_s \bar{u}_s \theta_s) \right] = (-p_s \bar{I} + \bar{\tau}_s) : \nabla \bar{u}_s + \nabla \cdot (k_\theta \nabla \theta_s) - \gamma \theta_s + \chi_{gs} \quad (12)$$

where

$(-p_s \bar{I} + \bar{\tau}_s) : \nabla \bar{u}_s$ is the energy generation by the solid stress tensor

$k_\theta \nabla \theta_s$ is the diffusion of energy (k_θ is the diffusion coefficient)

$\gamma \theta_s$ is the collisional dissipation of energy

χ_{gs} is the energy exchange between the solid and gas phase

The diffusion coefficient for granular energy

$$k_{\theta_s} = \frac{150\rho_s d_p \sqrt{\theta_s \pi}}{384(1+e_{ss})g_{o,ss}} \left[1 + \frac{6}{5} \alpha_s g_{o,ss} (1+e_{ss}) \right]^2 + 2\rho_s \alpha_s^2 d_p (1+e_{ss}) g_{o,ss} \sqrt{\frac{\theta_s}{\pi}} \quad (12a)$$

The dissipation of energy due to collision

$$\gamma_{\theta_s} = \frac{12(1-e_{ss}^2)g_{o,ss}}{d_p \sqrt{\pi}} \rho_s \alpha_s^2 \theta_s^{3/2} \quad (12b)$$

The energy transfer between phases due to random fluctuations of particle velocity

$$\chi_{gs} = -3K_{gs}\theta_s \quad (12c)$$

Equation (12) is the expression for partial differential equation (PDE) granular temperature. By neglecting the convection and diffusion terms, the partial differential equation becomes an algebraic equation and it is known as algebraic granular temperature model. The algebraic model is simple and can be used in most cases to accelerate the convergence.

Turbulent predictions for the continuous phase are obtained using the standard $k-\varepsilon$ model supplemented with extra terms that include the inter-phase turbulent momentum transfer. Predictions for turbulence quantities for the dispersed phase are obtained using the Tchen theory of dispersion of discrete particles by homogeneous turbulence [12].

IV. NUMERICAL SIMULATION PROCEDURE

Our computational domain is a horizontal 3D pipe of length 100D. We investigated different pipe diameters: 30 mm and 50 mm. The CFD simulation of turbulent and unsteady gas-solid flow was done using euler-euler approach. The commercial software package, Fluent 6.3 which is based on the finite volume approach, was used for solving the set of governing equations. The phase-coupled SIMPLE algorithm is used to couple the pressure and velocity. The standard $k-\varepsilon$ epsilon model [13] with standard wall function was used to treat turbulence phenomena in both phases and kinetic theory of granular flow (KTGF) is used to close the momentum balance equation in solid phase. Gambit 2.3.16 is used to generate the geometry and meshing. The simulations are performed in Quad 2 Core CPU running at 2.93 GHz with 4 GB of RAM.

A. Boundary Conditions and Model Parameters

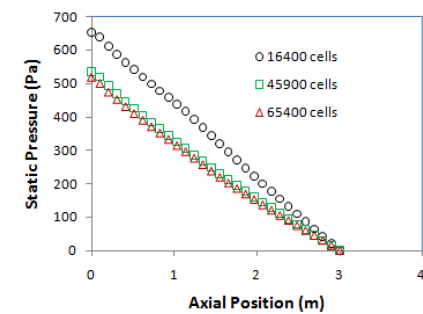
The particles enter the pipe into a developed gas flow field. So fully developed velocity profile ($1/7^{\text{th}}$ power law profile) is defined for gas phases and uniform velocity for solid phase at inlet along with the volume fraction of the solid phase.

$$\frac{U}{U_c} = \left(1 - \frac{r}{R}\right)^{1/7} \quad (13)$$

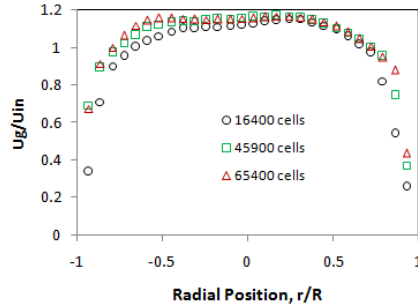
$$I_g = 0.16(Re_g)^{1/8} \quad (14)$$

An outflow boundary condition is used at the end of the pipeline, which obeys fully developed flow conditions where the diffusion fluxes for all flow variables in the direction of the flow are zero. For the wall boundary, no-slip condition is used for gas phase. Johnson and Jackson [14] boundary condition is used for particles to take into account the particle-wall collision and particle rebound. A value of 0.95 is set for coefficient of restitution for particle-wall collisions.

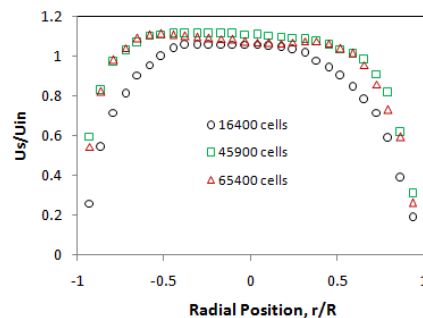
Grid independence test was carried out for 30 mm diameter pipe using 3 grids of mesh sizes 16400, 45900 and 65400 cells respectively. The solution has been verified to be grid independent with 45900 cells by checking that an increase in the number of grid points had a negligible effect on the computed profiles of pressure drop and velocity profiles.



(a)



(b)



(c)

Fig.1 Grid independence test for (a) axial pressure variation (b) Gas velocity profile (c) solid velocity profile

B. Monitoring the Variables

In gas–solid simulation, it is important to monitor the important flow parameters like solid velocity and volume fraction at outlet. Measurements should be taken in the statistical steady state regime when the variables reach steady state or statistical steady state regime.

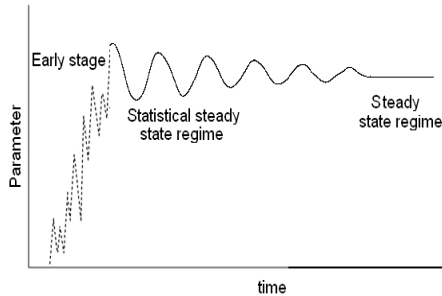
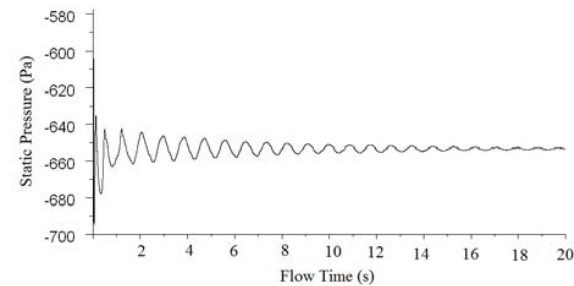
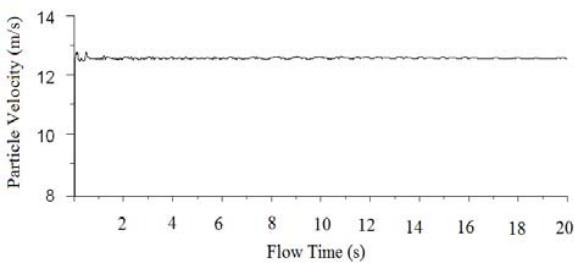


Fig. 2 Behavior of any parameter as predicted from a two-fluid transient simulation

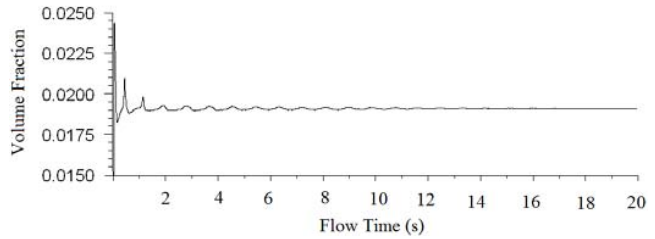
Fig. 2 illustrates the behavior of any parameter as predicted from a two-fluid transient simulation of the gas–solid flow [15]. From a given initial condition, the simulation goes through an early stage, and finally reaches the so-called statistical steady state regime. For practical purposes, this regime is considered reached when flow parameters start to oscillate around well defined means. If the behavior of the flow variable becomes a straight line, it is said to be reached steady state regime. Our predictions are in the statistical steady state regime as well as in the fully developed regions.



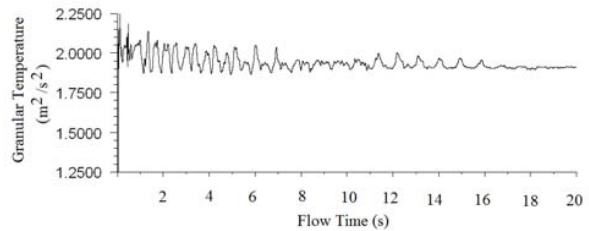
(a)



(b)



(c)



(d)

Fig.3 Time averaged values of flow parameters at outlet for $\rho_s = 1700 \text{ kg/m}^3$, $d_p = 100 \text{ micron}$, $\alpha = 0.02$, $U_g = 15 \text{ m/s}$

Fig. 3 shows the behavior of some of the flow parameters with flow time. We observe that 20s of simulation time is sufficient enough for the flow to be in steady state regime.

V. RESULTS AND DISCUSSION

A. Comparison with Experiment

The two fluid model predictions are compared for few cases against experimental findings of Tsuji et al. [10]. In their experiments, they used a 30 mm diameter pipe; particle diameter is 200 micron and density 1020 kg/m^3 . The mean velocity of gas (U_m) was varied from 6 to 20 m/s. First we simulate the flow neglecting the effect of lift and taking granular temperature as algebraic. In algebraic granular temperature model, particle-wall collision is also neglected.

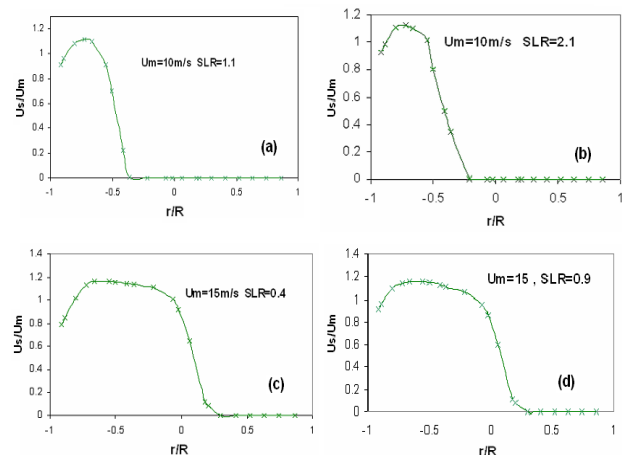
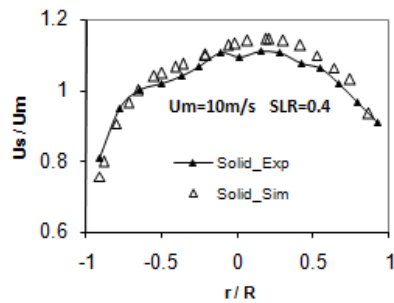


Fig.4 Velocity profiles of solid phase neglecting lift and particle-wall collision

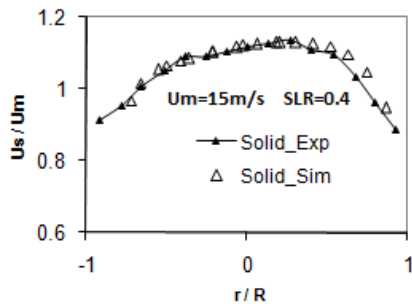
The velocity profiles for solid phase are plotted radially at outlet for different mean velocity and loading ratios. Figure 4 shows that solids are moving in the lower portion of the pipe and most of the upper portion is particle less zone. At higher velocities, particles try to suspend more and more towards the upper portion of the pipe. The mean velocities are more than the saltation velocity. So the solids are supposed to have suspended throughout the cross section in fully developed conditions as observed in the experiments. The results don't match well with the experimental findings.

B. Effect of Lift and Particle-Wall Collision

The problem with our preliminary investigation is the absence of lift and particle-wall collision in the simulation. In wall bounded gas solid flows, particles experience a phenomena called Magnus lift effect that arises due to the rotation of the particle [16]. The rotation takes place as a result of inter-particle as well as particle-wall collisions. Hence we consider the effect of lift (lift coefficient = 0.2) and particle-wall collision (restitution coefficient= 0.95) to reproduce the results of Tsuji et al. [10].



(a)



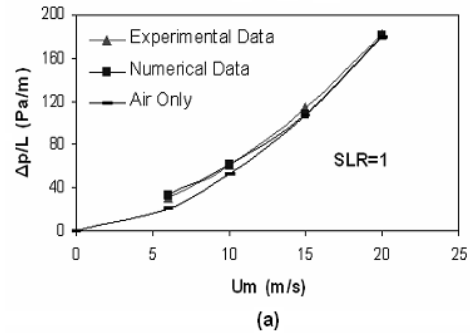
(b)

Fig.5 Comparison of normalized velocity curves.

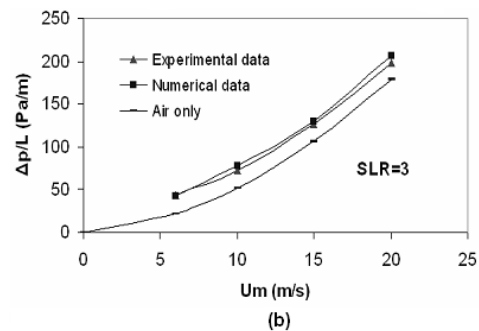
Now the predicted results are closely in good agreement with the experimental results. The gas velocity is always higher than the solid velocity. A little asymmetry is found in horizontal flow velocity profiles. This is due to the tendency of the particle to settle down due to gravity. The gravitational force makes the flow more complicated in the horizontal pipe than in the vertical one, as was mentioned by Owen [17]

Then we try to predict the pressure drop keeping all the model parameters constant and varying the specularly

constant. This is a factor measuring the particle-wall collision momentum loss. We try to match the numerical predictions with the experimental data for pressure drop by changing the value of specularly coefficient from zero and then go on increasing. We got good agreement between the experimental and numerical data at specularly coefficient equal to 0.08. The two phase pressure drop is always more than the gas only pressure drop for higher loadings.



(a)



(b)

Fig.6 Comparison of pressure drop prediction.

VI. EFFECT OF INFLUENCE PARAMETERS ON PRESSURE DROP

There are many factors affecting the behavior of gas solid flow like gas velocity, particle properties and particle loading. The dynamics of gas-solid flow in a horizontal pipe is strongly influenced by these parameters.

A. Effect of Inlet Gas Velocity

In pneumatic conveying, the gas flow exerts drag and hence the particles are getting transported along the pipe. Hence the inlet gas velocity is an important parameter in gas solid flows. From our numerical experiment considering different pipe diameter, particle properties and volume fraction, we observe that pressure drop increases with increase in gas velocity.

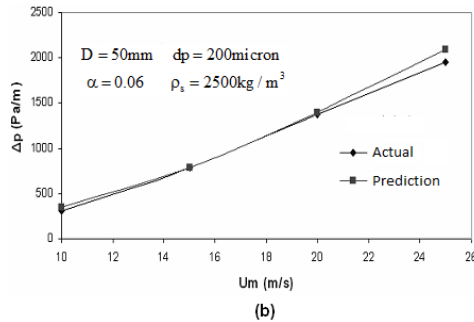
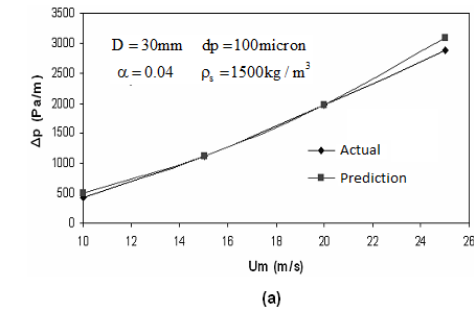


Fig.7 Pressure drop variation with mean gas velocity

We know that gas only pressure drop is proportional to square of the gas velocity. With base case of $U=15$ m/s, we also found that two phase pressure drop is also proportional to U^2 (with an error margin of $\pm 5\%$).

B. Effect of Particle Properties

Particle diameter and particle density are the two important terms appearing in the momentum equation. In industrial pneumatic conveying systems, the same type of material or various materials are commonly transported which have different sizes and densities. The effects of particle diameter on pressure drop were studied by changing them from 35 to 150 micron, keeping all other parameters constant. We investigated the results for a constant pipe diameter (30mm) and also for different pipe diameters. The pressure drop increases rapidly with increase in particle diameter, reach the peak value and then start decreasing.

The particle diameter is related to solids pressure, stress-strain tensor, and interaction forces, which determines the pressure. An increase in particle diameter causes a decrease in drag force, but the correlation among the particle diameter and solids pressure and stress-strain tensor is complex. After one critical value of particle diameter, the effect on drag force is dominant, so the pressure will decrease with increase in particle diameter.

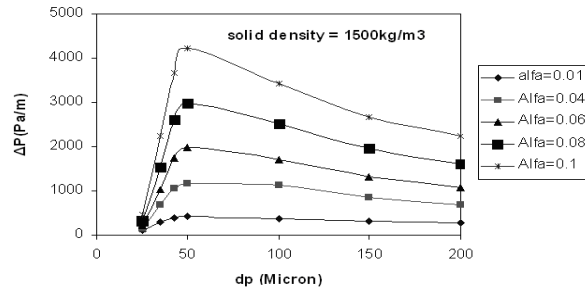


Fig.8 Effect of particle diameter on pressure drop for 30 mm pipe

For different pipe diameters, the similar trend is observed. As the pipe diameter increases, the pressure drop decreases. This behavior is similar to the single phase gas only flows. The peak reaches at different particle diameters for different pipe diameters, which is at 50 micron for a 30 mm diameter pipe. They begin to decrease and show a slight flattening with increase in particle diameter with a value greater than the peak.

The variation of pressure drop with particle density is shown in Fig.9 for different solid volume fractions (alfa). The pressure drop increases with particle density.

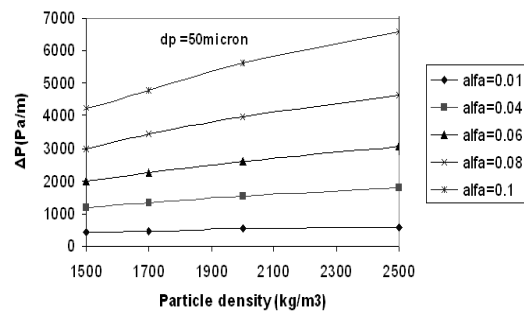


Fig.9 Pressure profiles with particle density at different volume fractions for 30mm diameter pipe

As the particle loading or volume fraction increases, the pressure drop along the pipe increases. Increasing particle loading or volume fraction increases the number of particle collisions in the pipe and in turn increasing the pressure drop. Singh and Simon [18] investigated the DEM simulation and suggested that though the total number of collisions increases with increasing particle loading, the increase of number of particle-particle collisions is greater than the increase of wall-particle collisions.

VII. CONCLUSION

The numerical simulation using Euler-Euler approach was performed for gas solid flows in horizontal pipes accounting for particle-wall and inter-particle collisions i.e. considering the so called four way coupling. The numerical results for velocity profiles and pressure drop profiles are validated against the experimental data of Tsuji et al. (1982). Excellent agreement was found by the numerical simulation with PDE granular temperature model and considering lift and particle-

wall collision. The lift force may be very less compared to the drag force, but cannot be neglected in the numerical simulation of gas solid flow in a horizontal pipe. We investigated the effect of variation of several parameters like particle size, mass loading, and density of the particle and also the velocity of transport on pressure drop prediction. The pressure loss increases with mean gas velocity, solid density, solid volume fraction and loading ratio. Pressure drop profile shows the same qualitative behavior with respect to volume fraction and solid loading ratio. With respect to particle diameter, pressure drop first increases, reaches a peak and then decreases.

REFERENCES

- [1] M. Sommerfeld, Analysis of collision effects for turbulent gas-particle flow in a horizontal channel: Pt 1. Particle transport. *Int. J. Multiphase Flow*, vol.29, no.4, pp. 675–699, 2003.
- [2] D. Gidaspow, *Multiphase Flow and Fluidization: Continuum and Kinetic Theory Descriptions*. Academic Press, Boston, 1994.
- [3] G.H. Yeoh and J. Tu, *Computational Techniques for Multi-Phase Flows: Basics and Applications*. Elsevier Science & Technology, Amsterdam, 2010.
- [4] M. Bohnet and O. Triesch, Influence of particles on fluid turbulence in pipe and diffuser gas-solid flows. *Chem. Eng. Technol.*, vol. 26, pp. 1254–1261, 2003.
- [5] J. Cao and G. Ahmadi, Gas-particle two-phase turbulent flow in a vertical duct. *Int. J. Multiphase Flow*, vol.21, no.6, pp.1203–1228, 1995.
- [6] Y. Zhang and J.M. Reese, Particle-gas turbulence interactions in a kinetic theory approach to granular flows. *Int. J. Multiphase Flow*, vol.27, pp.1945–1964, 2001.
- [7] Y. Zhang and J.M. Reese, Gas turbulence modulation in a two-fluid model for gas-solid flows. *AIChE Journal*, vol.49, no.12, pp.3048–3065, 2003.
- [8] C.T. Crowe, On models for turbulence modulation in fluid-particle flows. *Int. J. Multiphase Flow*, vol.26, pp.719–727, 2000.
- [9] K. Hadinoto and J.S. Curtis, Effect of interstitial fluid on particle-particle interactions in kinetic theory approach of dilute turbulent fluid-solid flow. *Ind. Eng. Chem. Res.*, vol.43, pp.3604–3615, 2004.
- [10] Y. Tsuji and Y. Morikawa, LDV measurements of an air-solid two-phase flow in a horizontal pipe. *J. Fluid Mech.*, vol.120, pp.385–409, 1982.
- [11] C.K.K. Lun, S.B. Savage, D.J. Jeffrey and N. Chepurmy, Kinetic theories for granular flow: Inelastic particles in couette flow and slightly inelastic particles in a general flow field. *J. Fluid Mech.*, vol.140, pp.223–256, 1984.
- [12] J. O. Hinze, *Turbulence*, McGraw-Hill Publishing Co., New York, 1975.
- [13] B.E. Launder and D.B. Spalding, The numerical computation of turbulent flows. *Computer Methods in Applied Mechanics and Engineering*, vol.3, pp.269–289, 1974.
- [14] P.C. Johnson and R. Jackson, Frictional-Collisional Constitutive Relations for Granular Materials, with Application to Plane Shearing, *J. Fluid Mech.* Vol.176, pp.67–93, 1987.
- [15] K. Agrawal, P.N. Loezos, M. Syamlal and S. Sundaresan, The role of meso-scale structures in rapid gas–solid flows. *J. Fluid Mech.*, vol.445, pp. 151–185, 2001.
- [16] C.T. Crowe, M. Sommerfeld and Y. Tsuji, *Fundamentals of Gas particle and Gas – Droplet Flows*. CRC Press, USA, 1998.
- [17] P.R. Owen, Pneumatic transport. *J. Fluid Mech.*, vol.39, pp.407–432, 1969.
- [18] V. Singh and L. Simon, Predicting pressure drop in pneumatic conveying using the discrete element modeling approach, *Seventh International Conference on CFD in the Minerals and Process Industries*, Melbourne, Australia, 2009.